Modular Approach for the Optimal Wind Turbine Micro Siting Problem through CMA-ES Algorithm

Sílvio Rodrigues
Electrical Power Processing
Mekelweg 4 2628 CD
Delft, The Netherlands
s.m.fragosorodrigues@tudelft.nl

Pavol Bauer
Electrical Power Processing
Mekelweg 4 2628 CD
Delft, The Netherlands
p.bauer@tudelft.nl

Jan Pierik
Energy Research Centre
of the Netherlands (ECN)
Petten, The Netherlands
pierik@ecn.nl

ABSTRACT

Although, only in recent years, northern European countries started to install large offshore wind farms, it is expected that by 2020, several dozens of far and large offshore wind farms (FLOWFs) will be built in the Baltic, Irish and North seas. These FLOWFs will be constituted of a considerable amount of wind turbines (WTs) packed together, leading to an energy density increase. However, due to shadowing effects between WTs, power production is reduced, resulting in a revenues decrease. Therefore, when FLOWFs are considered, wake losses reduction is an important optimization goal. This work presents a modular approach to optimize the energy yield of FLOWFs through an evolutionary algorithm. In order to do so the algorithm is set to find an optimal WF layout. The method consists of a modular strategy where the site wind rose information is used in different steps, which accelerates the calculation speed of the wake losses. The results presented demonstrate the method effectiveness. A computational time decrease is observed when compared to the standard optimization strategy, without jeopardizing the quality of the optimal layouts achieved.

Categories and Subject Descriptors

G.1.6 [**Optimization**]: Global optimization

General Terms

Algorithms, Performance

Keywords

CMA-ES, Modular Approach, Optimization, Turbine Micro Siting, Wake Losses, Wind Energy

1. INTRODUCTION

According to the European Commission, offshore wind will have a substantial contribution in helping the European Union to meet its energy policy objectives. Hence, a substantial increase in the offshore wind installed capacity is expected in the coming years. This growth, when compared to the current installed capacity, is believed to be approximately 30 to 40 times higher, by 2020, and 100 times in 2030 [1]. Together with the wind farms (WFs) rated power, also the average number of installed turbines per WF is rapidly increasing, as shown in Figure 1. Furthermore, it is believed that this trend will continue [2].

In order to reduce costs, e.g. internal collection system cost, turbines tend to be packed in WFs. However, the installation of wind turbines (WTs) close to each other causes interferences such as shadowing effects. For example, the efficiency of the Danish Horns Rev offshore wind farm is 11% lower when compared to what the same turbines would produce if installed alone [4]. Thus, it is important to reduce the wake losses in far and large offshore wind farms (FLOWFs). Optimizing the WT micro siting is one possible strategy to reduce wake losses. However, due to the high nonlinearity nature and amount of design variables of the problem, the search space becomes too complex to be solved through deterministic algorithms. A possible solution is the use of stochastic algorithms, where randomness is included in the process [5].

The use of optimization methods inspired by biological processes in the WT micro siting problem is not novel. For instance, an evolutive algorithm set to optimize the WF profits was used in [6]. In order to do so, it was required the minimization of the investment costs while maximizing the net cash flows, through energy

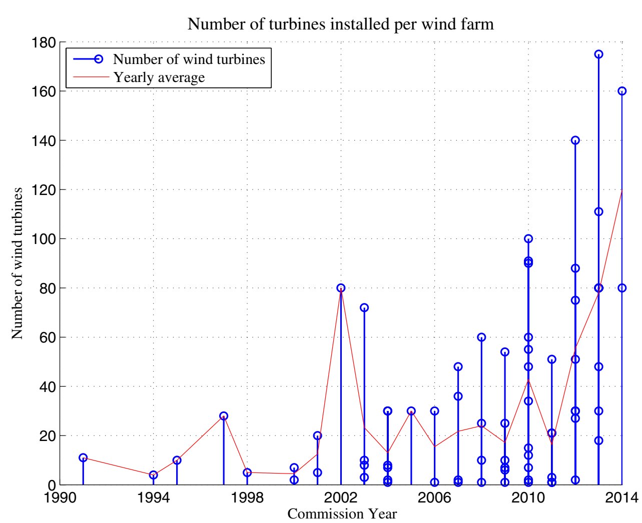

Figure 1: Evolution of the wind turbines number per offshore wind farm and the yearly average [3].

generation optimization and power losses reduction. Discrete and continuous variables were considered, making the optimization an integer-mixed type problem. An analytical optimization framework for offshore WF layout optimization problems, using the energy levelized cost as objective function, is presented in [7]. In this method, for each WT, the Weibull scale parameters are corrected in order to account for the wake losses. A modular and parallelizable evolutionary optimization strategy set to optimize the layout of a WF with thousand turbines is presented in [8]. In addition, the wake losses scaling with the number of turbines is analyzed.

An approach for the turbine micro siting problem that transforms the WF area into a finite grid is used in [9]. A "lazy greedy" algorithm was employed. Additionally, the wake losses model was extended in order to handle complex terrain areas. A methodology named Unrestricted Wind Farm Layout Optimization (UWFLO) which covers several aspects regarding wind farm planning was suggested in [10]. The analytical wake losses model employed was originally proposed in [11]. In order to solve the single-objective problem – WF energy production maximization – a Particle Swarm Optimization (PSO) algorithm was used. To guarantee that the solutions were feasible, constraints regarding the minimum distance between neighboring turbines and maximum WF area were employed. The methodology was applied to different case scenarios with identical and non-identical WTs.

A multi-objective approach for energy capture maximization and turbine and land area cost minimization is presented in [12]. The PSO was the algorithm implemented and wake losses were considered. In [13] the optimization problem for maximizing the WF energy output was also solved in a multi-objective manner. The constraint violation was considered as a second objective to be minimized.

The objective of the study performed in [5] was to investigate different optimization algorithms applied in offshore WF micro siting problems. Five optimization algorithms, viz. gradient search algorithm (GSA), greedy heuristic (GH), genetic algorithm (GA), simulated annealing (SA) and pattern search (PS), were evaluated and compared in respect to their applicability and performance in WF micro siting problems.

This work presents a modular approach to optimize the energy yield of FLOWFs through an evolutionary algorithm. In order to do so the algorithm is set to find an optimal WT layout. The method consists of a modular strategy where the site wind rose information is used in different steps.

The sections of the paper are organized as follows: in the next section an introduction to wake losses modeling is given. Thereafter, the evolutionary algorithm employed is presented. In the following section, the proposed optimization method is described. Thereafter, a case study is presented, followed by the results section. A sensibility analysis is carried out and at the end conclusions are drawn.

2. WAKE LOSSES

In this work, the wake growth model used was proposed in [14], while the wind speed deficit model employed was originality presented in [15]. This model has been widely adopted in WF modeling [16]. More information regarding different analytical wake losses models, applicable for both small and large WFs, may be found in [17, 18, 19].

Differently from a solitary WT, the wind speed seen by a *j-th* turbine positioned in the wake of one or more turbines, is given by:

$$U_j = U_0\,(1 - deficit) \tag{1}$$

where U_0 is the ambient wind speed and $deficit$ is the velocity decrease caused by shadowing effects.

The wake expansion is considered to be linear, hence:

$$R_k^w = R_k + \alpha d_{kj} \tag{2}$$

where R_k^w is the wake front radius, R_k is the turbine rotor radius, α is the decay factor – in offshore conditions, a value of 0.05 is normally used [19] – and d_{kj} is the distance between the turbines being considered.

The interference caused by an upstream *k-th* turbine to the *j-th* turbine may be calculated as:

$$U_{kj} = \frac{1-\sqrt{1-C_{T_k}}}{\left(1+\frac{\alpha d_{kj}}{R_j}\right)^2}\frac{A_{kj}}{A_j} \tag{3}$$

where C_{T_k} is the *k-th* turbine thrust coefficient at a given speed, A_j is the *j-th* turbine rotor area and A_{kj} is the *j-th* turbine rotor area influenced by the upstream turbine *k*.

If the wake front affects entirely the *j-th* turbine, $A_{kj} = \pi R_j^2$. If the wake wave affects partially the turbine rotor sweep area (see Figure 2), A_{kj} is given by (4), shown in footnote. Finally, if the wake front does not impact the *j-th* turbine, $A_{kj} = 0$.

The wake losses model takes into consideration multiple interferences from WTs located upstream. Hence, the deficit term is calculated as:

$$deficit = \sqrt{\sum_{k=1}^{n} U_{kj}^2} \tag{5}$$

Assumptions

Several assumptions were made in the wake speed deficit modeling. These assumptions may lead towards results that may not rep-

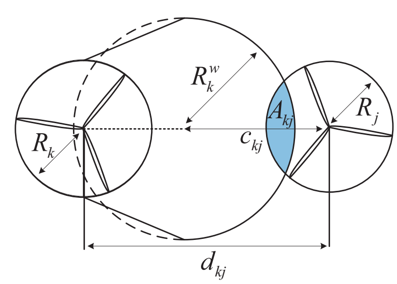

Figure 2: Wind turbine partially affected by an upstream turbine wake front.

$$A_{kj} = \frac{1}{2}\left(R_k^{w2}\left(2\arccos\left(\frac{R_k^{w2}+c_{kj}^2-R_j^2}{2R_k^w c_{kj}}\right) - \sin\left(2\arccos\left(\frac{R_k^{w2}+c_{kj}^2-R_j^2}{2R_k^w c_{kj}}\right)\right)\right) + R_j^2\left(2\arccos\left(\frac{R_j^2+c_{kj}^2-R_k^{w2}}{2R_j c_{kj}}\right) - \sin\left(2\arccos\left(\frac{R_j^2+c_{kj}^2-R_k^{w2}}{2R_j c_{kj}}\right)\right)\right)\right) \tag{4}$$

resent the reality. A Computational Fluid Dynamics (CFD) model is likely to achieve a more accurate estimation of the wake velocities [20]. However, a major disadvantage of such high fidelity CFD simulations is the excessive computational complexity and processing time. Such drawback is further heightened when evolutionary algorithms are used, since a high amount of function evaluation is required. In the following bullet points the assumptions made are described:

- The wind speed in the wake front is axi-symmetric;
- The wake front starts to expand after the turbine rotor;
- Linear wind speed reduction inside the wake front;
- Turbine loads and properties of the local terrain were not considered;
- The WTs are identical, i.e. similar physical and performance characteristics;
- Wind turbulence was not considered;
- The freestream wind speed is homogenous.

Due to the assumptions described above, it may be possible to achieve wind farm layouts where the energy production is increased as well as the turbulence felt by the turbines. In this way, it is important to verify how an optimized solution found with the simplified model performs in a more robust wake losses model, where turbine loads are also taken into consideration.

3. CMA-ES ALGORITHM

The covariance matrix adaptation evolution strategy (CMA-ES), originally designed for small populations [21], is one of the most powerful evolutionary algorithms for real-valued single-objective optimization of non-linear and non-convex functions [22, 23].

The CMA self-adapts the covariance matrix of a multivariate normal distribution, which is used to sample new solution from the multidimensional search space, where each variate is a search variable [8]. The correlations between the variable are respected due to the covariance matrix, making it a powerful evolutionary optimization algorithm [24].

The CMA is invariant against order-preserving transformations of the fitness function value and, disregarding initialization, also invariant against rotation and translation of the search space. If the strategy parameters are properly initialized or if the time needed to adapt the strategy parameters is neglected, any transformation of the search space does not affect the performance of the CMA [24].

The CMA algorithm has been applied in different fields of engineering [25]. In Figure 3 a flowchart of the CMA-ES algorithm is presented.

3.1 Initial Population

At the initialization, step 1 of Figure 3, an initial standard layout is created. The composition of a solution is given in (6). Encoded in the solutions are the turbine coordinates, which have as boundaries the WF area limit. All the encoded variables are real valued.

$$\mathbf{X} = \left[\begin{array}{cccccc} x_1 & \cdots & x_k & y_1 & \cdots & y_k \end{array}\right] \tag{6}$$

where (x_1, y_1) and (x_k, y_k) correspond to the coordinates of the first and k-th WTs, respectively.

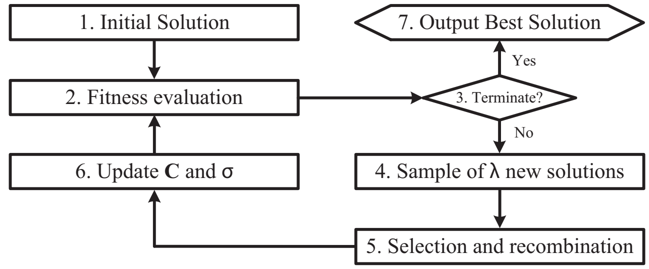

Figure 3: Flowchart of the CMA-ES algorithm.

3.2 Optimization goal

In step 2, the fitness function is evaluated. The optimization goal, wind farm efficiency, is expressed as:

$$\eta_{WF} = \frac{P_{WF}}{\sum_{i=1}^{n} P_{WT_i}} \tag{7}$$

where η_{WF} is the WF efficiency, P_{WF} is the WF total power production and $\sum_{i=1}^{n} P_{WT_i}$ represents the power produced by the turbines without shadowing effects. The WF efficiency optimization was performed through the minimization of $-\eta_{WF}$.

Constraints

In order to obtain feasible results for the optimal WT siting problem, the following constraints – displayed in Figure 4 – were implemented [10]:

- A minimum distance between neighboring turbines is required. In this work a minimum separation of four turbine rotor diameters was considered;
- The WTs have to be placed inside the WF area.

3.3 Stopping Criterion

The optimization will end and return the best individual in the population when the maximum number of generations is reached.

3.4 Sampling of new solutions

In the CMA-ES, a population of λ new individuals is generated by sampling a multivariate normal distribution:

$$\mathbf{x}_k^{(g+1)} \sim \mathbf{m}^{(g)} + \sigma^{(g)} N\left(0, \mathbf{C}^{(g)}\right) \text{ for } k = 1, ..., \lambda \tag{8}$$

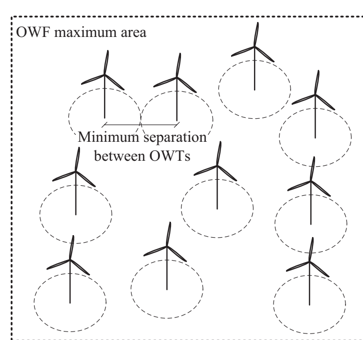

Figure 4: Problem constraints taken into consideration.

where $\mathbf{m}^{(g)}$ is the mean value of the search distribution at generation g, $\sigma^{(g)}$ is the standard deviation, $N\left(0, \mathbf{C}^{(g)}\right)$ is a multivariate normal distribution with zero mean and covariance matrix $\mathbf{C}^{(g)}$.

3.5 Selection and Recombination

In step 5, the best $\mu = \lfloor \lambda/2 \rfloor$ solutions are selected for recombination to obtain the new mean value of the search distribution. The CMA variant performs a comma-selection, meaning that no elitism is performed, which enhances the escape from local minima of the problem [23].

$$\mathbf{m}^{(g+1)} = \sum_{i=1}^{\mu} w_i x_{i:\lambda}^{(g+1)} \tag{9}$$

where $\mu \leq \lambda$ is the number of selected points, $w_{i=1\ldots\mu}$ are the weight coefficients for recombination which respect: $\sum_{i=1}^{\mu} \omega_i = 1, \omega_i > 0$.

3.6 Update C and σ

In order to update the covariance matrix, $\mathbf{C}$, it is first necessary to update the evolution path, given by:

$$\mathbf{p}_c^{(g+1)} = (1 - c_c)\,\mathbf{p}_c^{(g)} + \sqrt{c_c\,(2 - c_c)\,\mu_{eff}}\,\frac{\mathbf{m}^{(g+1)} - \mathbf{m}^{(g)}}{\sigma^{(g)}} \tag{10}$$

where $\mu_{eff} = \left(\sum_{i=1}^{\mu} w_i^2\right)^{-1}$.

Thereafter, $\mathbf{C}$ is updated according to:

$$\mathbf{C}^{(g+1)} = (1 - c_1 - c_\mu)\,\mathbf{C}^{(g)} + c_1 \mathbf{p}_c^{(g+1)} \mathbf{p}_c^{(g+1)^T} + c_\mu \sum_{i=1}^{\mu} w_i \mathbf{y}_{i:\lambda}^{(g+1)} \left(\mathbf{y}_{i:\lambda}^{(g+1)}\right)^T \tag{11}$$

where $\mathbf{y}_{i:\lambda}^{(g+1)} = \dfrac{\left(\mathbf{x}_{i:\lambda}^{(g+1)} - \mathbf{m}^{(g)}\right)}{\sigma^{(g)}}$.

The standard deviation of the multivariate normal distribution is also updated. Firstly, the conjugate evolution path is updated:

$$\mathbf{p}_\sigma^{(g+1)} = (1 - c_\sigma)\,\mathbf{p}_\sigma^{(g)} + \sqrt{c_\sigma\,(2 - c_\sigma)\,\mu_{eff}}\,\mathbf{C}^{(g)^{-\frac{1}{2}}}\,\frac{\mathbf{m}^{(g+1)} - \mathbf{m}^{(g)}}{\sigma^{(g)}} \tag{12}$$

Finally, the standard deviation is updated through:

$$\sigma^{(g+1)} = \sigma^{(g)} \exp\left(\frac{c_\sigma}{d_\sigma}\left(\frac{\left\|\mathbf{p}_\sigma^{(g+1)}\right\|}{\sqrt{n}\left(1 - \frac{1}{4n} + \frac{1}{21n^2}\right)} - 1\right)\right) \tag{13}$$

The parameters used in the CMA-ES were set to their default values [23], while the initial values were set as: $\mathbf{C}^{(0)} = \mathbf{I}$, $\mathbf{p}_\sigma{}^{(0)} = \mathbf{p}_c{}^{(0)} = \mathbf{0}$ and $\sigma^{(0)} = 0.5$.

4. OPTIMIZATION METHODS

In this section, the modular and the standard optimization methods are introduced and compared.

4.1 Modular Optimization

The proposed optimization scheme is composed of three steps, as shown in Figure 5. The first step starts by placing the WTs in a standard configuration. Moreover, only the main wind direction is used to optimize the WTs siting problem. In this way, the wake losses evaluation computation burden is reduced.

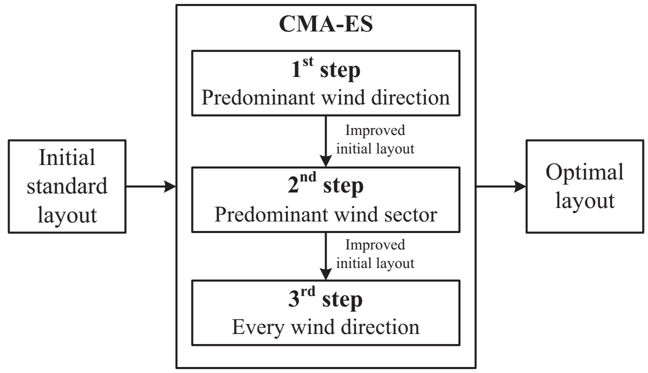

Figure 5: Proposed Modular Optimization Method.

In the second step, the WTs are placed in the best layout found in step 1. In this phase, the main wind sector is considered, leading to higher wake losses evaluation times. However, a higher model accuracy is obtained.

In the third and last optimization stage, similarly to step 2, the turbines are placed in the best layout found in the previous step. The entire wind rose is now used. Hence, the wake losses model is slower but it offers maximum accuracy.

It is important to refer that the multi-scale approach to solve the wind turbine micro siting problem introduced in this work prevails, independently of the optimization algorithm used.

4.2 Standard Optimization

The standard optimization is considered to be the technique of optimizing the offshore WF layout through a CMA-ES algorithm. Differently from the proposed method, the complete wind rose information is used throughout the entire optimization process. The initial turbine layout is similar to the one used in step 1 of the proposed method.

5. CASE STUDY

In order to evaluate the wake losses, information regarding the wind is needed. In Figure 6 it is shown a wind rose with the average wind speeds and respective frequencies. Moreover, the wind directions considered in the first and second steps of the proposed optimization method are highlighted.

For the present case study, the WF was considered to have a square shape, with 5 km per side, 36 identical turbines and an installed capacity of 221.4 MW. Initially the turbines were placed in a grid with 1 km distance between them.

The turbines, used in this work, have a hub height of 100 m and a 126 m rotor dimater. Figure 7 presents the power curve of a single turbine and the fitted function. The thrust coefficient for the operational wind speeds and the respective fitted function are shown in Figure 8. The curve fitting was required since the power and thrust values are needed for a continuous range of wind speeds.

The fairest manner to compare the methods is by giving the same processing time to both strategies, since the standard method would require a longer period of time to run the same amount of generations. The modular optimization approach was set to run for 350 generations. Both methods were simultaneously terminated once the proposed method completed the preestablished iterations.

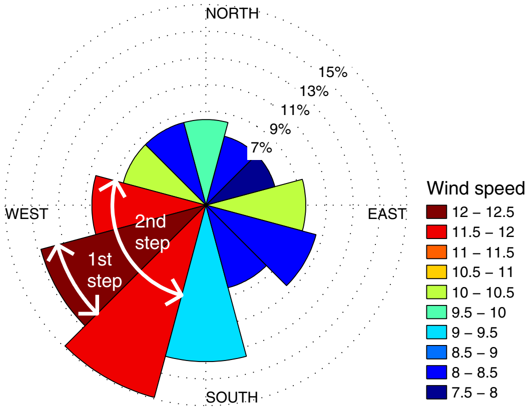

Figure 6: Wind rose with the average wind speeds and frequencies.

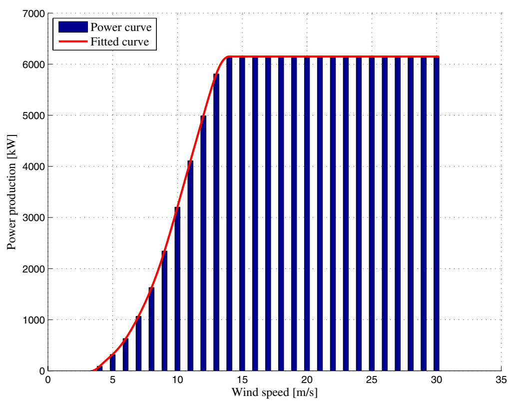

Figure 7: Wind turbine power curve.

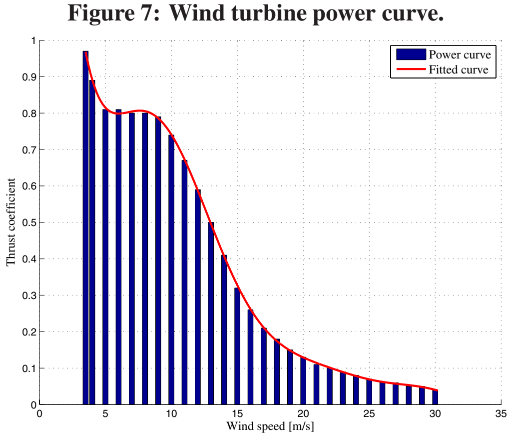

Figure 8: Wind turbine thrust curve.

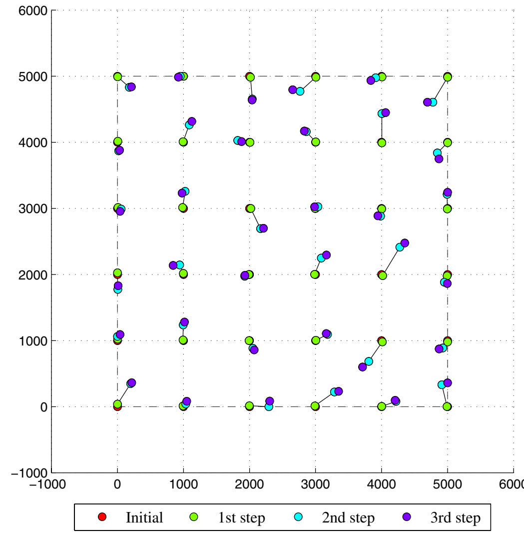

Figure 9: Initial and final layouts for the modular optimization method.

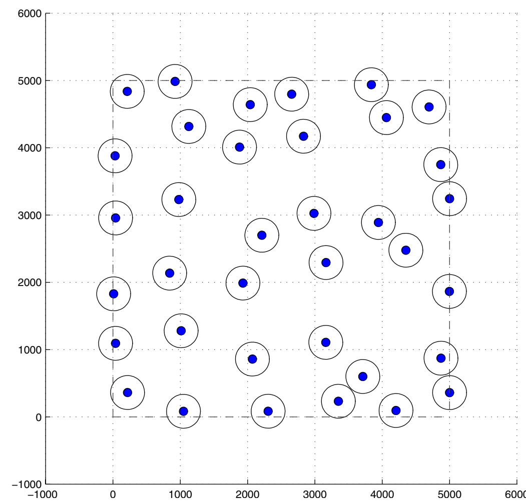

Figure 10: Optimal layout with the minimum distances between WTs.

6. RESULTS

6.1 Proposed Optimization

Figure 9 shows the initial and final turbine layouts of all optimization steps, while in Figure 10 the final optimal layout and the minimum distance between neighboring WTs are presented. In Figure 9, it can be seen that in the first step, the turbines coordinates did not differ much from the initial layout. On the other hand, the highest variation occurred during the second step, since in the third and last step, the turbines, once again, were not placed far from their initial coordinates.

In Table 1, for each optimization step, the initial and final fitness values, the processing time and the number of generations are shown. The first step only improved circa 0.05% the wind farm efficiency. It is possible to conclude that considering only the main wind direction is not representative of the entire wind rose.

A pre-established number of generations were given to each step. However, the optimal number of generations to be attributed to each step is rather complicated to obtain. Another approach that may be suitable, is to move to the next step after a certain number of iterations whiteout further improving the fitness value.

6.2 Standard Optimization

In Figure 11 the initial and final WT layouts found are depicted. In Table 2, the initial and final fitness values, the processing time and the number of generations are shown.

Table 1: **Run time, Iterations number and fitness values.**

Step	Fitness value [%]		Time [s]	Generations
1	80.77	80.83	4.67	50
2	80.83	90.28	45.37	200
3	90.28	92.49	86.46	100

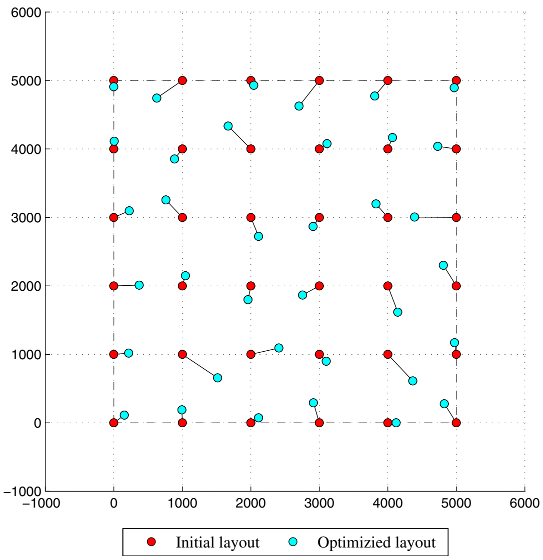

Figure 11: Initial and optimized layout for the standard optimization process.

Table 2: Run time, Iterations number and fitness values.

Step	Fitness value [%]		Time [s]	Generations
1	80.77	90.9	136.8	144

6.3 Comparison

In this section a comparison between the results obtained with the two optimization methods is performed.

Figure 12 shows the best fitness values during both optimizations. For the proposed method the wind farm efficiency was recaculculated in order to considered the entire wind rose (green curve). This is why the efficiency presents lower values during the optimization. On the other hand, the blue curve represents the wind farm efficiency seen by the algorithm during the optimization.

It is possible to observe that, when the proposed method advances to the next step, the fitness value drops. The WF layout performs worse with new wind directions since they were not taken into consideration previously. The highest fitness value drop, circa 9%, was observed when the method completed the first step (see Table 1). On the other hand, a decrease of approximately 6% was observed once the algorithm entered the last optimization step.

During the second step of the proposed method, it can be seen that the same curve shape can be found in the blue and green curves. For this wind rose, it can be concluded that, even though only 25% of the wind information is being used, the wake losses are, to some extent, representative for the entire wind rose.

The highest WF efficiency achieved with the standard method was 90.9% (see Table 2). This fitness value was obtained with the proposed method within approximately 93 s. Therefore, the proposed method only required circa 32% of the processing time to reach the same WF efficiency.

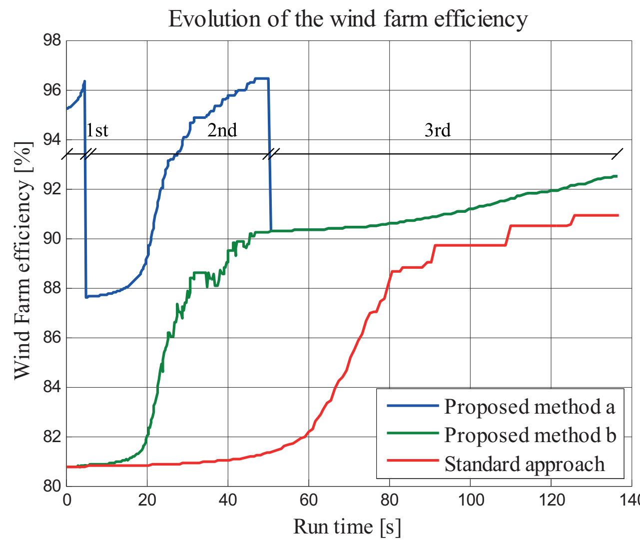

Figure 12: Best found fitness values during optimization for both strategies.

The average iteration time was 0.39 s for the proposed approach and 0.95 s for the standard optimization method. This result may be explained by the fact that, in the first two steps of the proposed method, only a fraction of the wind directions were considered. Hence, the wake losses evaluation is performed with a lower computational requirement, leading to a iteration speed decrease.

7. SENSITIVITY ANALYSIS

The construction of an offshore WF represents a huge investment made by, usually, an entity consortium. Therefore, an usual requirement is a sensitivity study in order to avoid unwanted project outcomes. For instance, as shown in Figure 13, it is preferable to obtain a local maximum for the WF layout problem, which is stable when facing layout uncertainties, rather than a global maximum which shows a high sensitivity to variations.

7.1 Turbine siting variation

In the first part of the sensitivity analysis, the WTs positions were independently perturbed in a total of ten thousand times. The random WT coordinates were sampled from a two-variable normal distribution, which has as mean values the initial coordinates of the turbine and a covariance matrix given by:

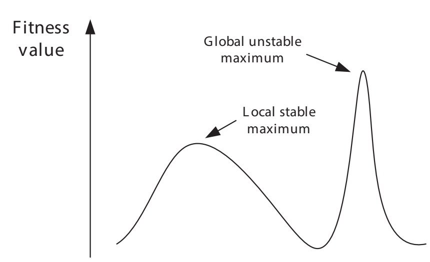

Figure 13: Local and global maximum of a function with different sensitivities.

$$\mathbf{C} = \begin{bmatrix} 20 & 0 \\ 0 & 20 \end{bmatrix} \quad (14)$$

Figure 14 displays the probability density function for the initial layout and for both optimal layouts. It is possible to observe that the initial layout has the lowest standard deviation, $\sigma = 0.019$, and the lowest wind farm efficiency mean, $m = 80.77\%$. This means that the initial layout is the one that offers the lowest sensitivity to misplacement of turbines in the wind farm.

The optimal layouts found with the standard and proposed methods have similar standard deviations, $\sigma = 0.052$ and $\sigma = 0.036$, respectively. Regarding the mean values the layout found with the proposed method has the highest mean value, $m = 92.46\%$.

7.2 Wind rose variation

In the second part, the wind rose was perturbed in order to verify the sensitivity of the layouts. Both the mean wind speeds and frequency for all directions were altered. In order to do so, random numbers sampled from a normal distribution were added to the initial values:

$$\begin{cases} (\text{wind speed})_\theta = (\text{wind speed})_\theta + \mathcal{N}\ (0, 0.1) \ \text{for}\ \theta = 0, \ldots, 360^\circ \\ (\text{wind frequency})_\theta = (\text{wind frequency})_\theta + \mathcal{N}\ (0, 0.1) \ \text{for}\ \theta = 0, \ldots, 360^\circ \end{cases} \quad (15)$$

In Figure 15 it is shown the probability density function for the initial layout and for both optimal layouts. The initial layout presents the highest standard deviation, $\sigma = 0.342$, while the layout obtained with the proposed method has the lowest standard deviation, $\sigma = 0.132$. Hence, the layout obtained with the proposed optimization method is the one that is the least affect if variations occur to the wind rose.

With the performed sensitivity study, it can be concluded, that although the optimal layouts present a higher sensitivity to perturbations to the turbine coordinates, the variation that might outcome from such misplacement does not affect gravely the wind farm efficiency. Furthermore, the optimal layouts have a lower sensitivity to perturbations made to the wind rose, when compared to the initial layout.

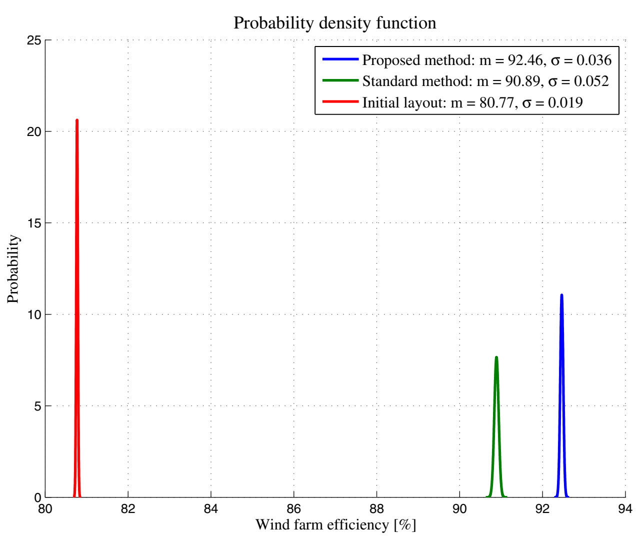

Figure 14: Probability density functions obtained for the turbine coordinates perturbation.

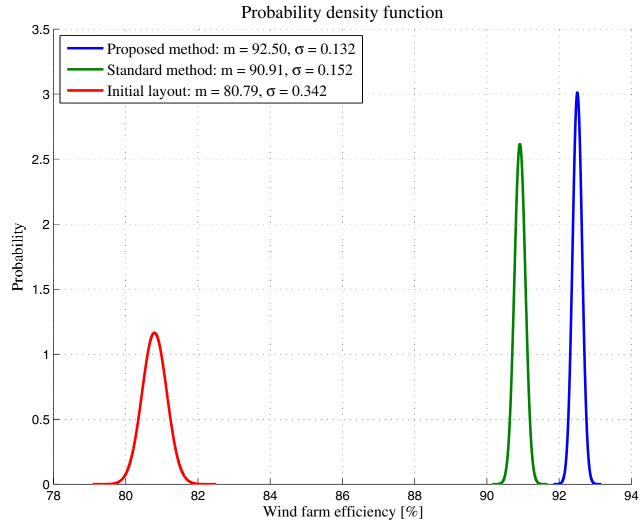

Figure 15: Probability density functions obtained for the wind rose perturbation.

8. CONCLUSIONS

Future FLOWs will be built with a higher number of turbines packed in a constricted area. Thus, wake losses will play an important role in the energy capture efficiency. A modular optimization framework for the turbine layout problem was introduced.

The optimization method proposed in this work, due to its modular approach, provides optimal wind turbine layouts with lower computational burden. Moreover, the method is independent of the wake losses model and optimization algorithm. However, since multiple wake losses evaluations are required, the use of detailed wake losses models for optimization purposes becomes prohibitive.

As future work it would be interesting to verify and investigate how layouts found with the proposed optimization method would perform with more accurate wake losses models.

9. ACKNOWLEDGEMENTS

The work has been performed within the project "Far and Large Offshore Wind (FLOW)". The project is supported by the Ministry of Economic Affairs, Agriculture and Innovation of the Netherlands within the EOS-LT program of Agentschap-NL (P201101-005-ECN). The opinion expressed by the authors do not necessarily reflect the position of the Ministry of Economic affairs, nor does it involve any responsibility on its part.

10. REFERENCES

[1] European Commission. (2008) [Last accessed 1st March 2013]. [Online]. Available: http://eur-lex.europa.eu/LexUriServ/LexUriServ.do?uri=CELEX:52008DC0768:EN:HTML

[2] EWEA, "The European offshore wind industry key 2011 trends and statistics," EWEA, Tech. Rep. January, 2012.

[3] LORC. (2013) [Last accessed 9th March 2013]. [Online]. Available: http://www.lorc.dk/offshore-wind-farms-map/list

[4] T. Sorensen, M. L. Thogersen, and P. Nielsen, "Adapting and calibration of existing wake models to meet the conditions inside offshore wind farms," EMD International A/S, Tech. Rep., 2008.

[5] C. N. Elkinton, J. F. Manwell, and J. G. McGowan, "Algorithms for Offshore Wind Farm Layout Optimization," *Wind Engineering*, vol. 32, pp. 67–84, 2008.

[6] J. S. Gonzalez, G. G. Rodriguez *et al.*, "Overall design optimization of wind farms," *Renewable Energy*, vol. 36, no. 7, pp. 1973–1982, 2011.

[7] M. A. Lackner and C. N. Elkinton, "An Analytical Framework for Offshore Wind Farm Layout Optimization," *Wind Engineering*, vol. 31, pp. 17–31, January 2007.

[8] M. Wagner, K. Veeramachaneni *et al.*, "Optimizing the layout of 1000 wind turbines," in *European Wind Energy Association Annual Event*. Brussels, Belgium: European Wind Energy Association, 2011, pp. 1–10.

[9] Z. Changshui, H. Guangdong, and W. Jun, "A fast algorithm based on the submodular property for optimization of wind turbine positioning," *Renewable Energy*, vol. 36, no. 11, pp. 2951 – 2958, 2011.

[10] S. Chowdhury, J. Zhang *et al.*, "Unrestricted wind farm layout optimization (UWFLO): Investigating key factors influencing the maximum power generation," *Renewable Energy*, vol. 38, no. 1, pp. 16 – 30, 2012.

[11] S. Frandsen, R. Barthelmie *et al.*, "Analytical modelling of wind speed deficit in large offshore wind farms," *Wind Energy*, vol. 9, no. 1-2, pp. 39–53, 2006. [Online]. Available: http://dx.doi.org/10.1002/we.189

[12] K. Veeramachaneni, M. Wagner *et al.*, "Optimizing energy output and layout costs for large wind farms using particle swarm optimization," in *IEEE Congress on Evolutionary Computation*, 2012, pp. 1–7.

[13] A. Kusiak and Z. Song, "Design of wind farm layout for maximum wind energy capture," *Renewable Energy*, vol. 35, pp. 685–694, 2010.

[14] N. Jensen, "A note on wind generator interaction," Risø National Laboratory, Tech. Rep., 1983.

[15] I. Katic, J. Højstrup, and N. Jensen, *A Simple Model for Cluster Efficiency*. A. Raguzzi, 1987, pp. 407–410.

[16] A. Crespo, J. Hernández, and S. Frandsen, "Survey of modelling methods for wind turbine wakes and wind farms," *Wind Energy*, vol. 2, no. 1, pp. 1–24, 1999.

[17] R. J. Barthelmie, G. C. Larsen *et al.*, "Comparison of Wake Model Simulations with Offshore Wind Turbine Wake Profiles Measured by Sodar," *Journal of Atmospheric and Oceanic Technology*, vol. 23, no. 7, pp. 888–901, 2006.

[18] D. J. Renkema, "Validation of wind turbine wake models using wind farm data and wind tunnel measurements," Master's thesis, Delft University of Technology, June 2007.

[19] R. A. Rivas, "Optimization of Offshore Wind Farm Layouts," Master's thesis, Technical University of Denmark, August 2007.

[20] B. Sanderse, "Aerodynamics of wind turbine wakes - literature review," Energy Research Centre of the Netherlands (ECN), Tech. Rep., 2009.

[21] N. Hansen, "The CMA Evolution Strategy: A Comparing Review," 2006.

[22] C. Igel, N. Hansen, and S. Roth, "Covariance Matrix Adaptation for Multi-objective Optimization," *Evolutionary Computation*, vol. 15, no. 1, pp. 1–28, 2007.

[23] N. Hansen, "The CMA Evolution Strategy: A Tutorial," Laboratoire de Recherche en Informatique, Tech. Rep., 2008.

[24] N. Hansen and S. Kern, "Evaluating the CMA Evolution Strategy on Multimodal Test Functions," in *Parallel Problem Solving from Nature*, vol. 3242. Springer, 2004, pp. 282–291.

[25] N. Hansen, 2009, Last accessed in 4 March 2013. [Online]. Available: https://www.lri.fr/~hansen/cmaapplications.pdf